MAGNETOHYDRODYNAMICS Vol. 46 (2010), No. 3, pp. 257–269

STRUCTURAL AND RHEOLOGICAL STUDY OF MAGNETIC FLUIDS USING MOLECULAR DYNAMICS

Taixiang Liu[1], *Rui Gu*[1], *Xinglong Gong*[1†], *Shouhu Xuan*[1], *Hengan Wu*[1], *Zhong Zhang*[2]

[1] *CAS Key Laboratory of Mechanical Behavior and Design of Materials, Department of Modern Mechanics, University of Science and Technology of China, Hefei, 230027, China*

[2] *National Center for Nanoscience and Technology, Beijing 100080, China*

In this study, molecular dynamics simulations based on a magnetic dipole theory were developed to study microstructural evolution, rheological properties and potential energies of magnetic fluids (MF) under steady shear or compression. In general, the magnetic interaction dipole forces drive the nanoparticles to form firstly a chain-like and then a column-like structure under an externally applied magnetic field. The potential energies are time-dependent and the static yield stresses increase with the growth of magnetic field strength. Under the steady shear, the one-dimensional chain or column structures would transform into lamellar patterns. The shear stresses were theoretically predicted and they agreed well with experimental results. Under compression, when magnetic fluids were compressed along the magnetic field, simulation results show that the materials exhibit enhanced yield stresses and the work of compressive loading is absorbed mostly by the repulsive potential energy.

Introduction. Magnetic fluids [1], a kind of colloidal suspension of magnetic nanoparticles, have attracted considerable interests due to their wide applications, such as magnetorheological technology, storage technology [2], biomedicine [3], etc. Due to their specific magnetic property, the rheological property of the magnetic fluids changes dramatically when an external magnetic field is applied. Recently [4, 5], experiences and theoretical analyses have been employed to investigate the microstructural evolution or rheological properties of magnetic fluids. These works indicate that the aggregations of magnetic particles are formed in suspensions and the shape, size and the quantitative distribution of the one-dimensional aggregates have significant influence on the rheological properties of magnetic fluids. In addition, experimental results [6] also demonstrate that the microstructures of magnetic particles indeed strongly affect their rheological properties. However, to the best of our knowledge, the mechanical property transformation based on the microstructural evolution has not been investigated. Because the aggregates have significant influence on the rheological properties, it is very important to investigate the characteristics of these micro-aggregates and how they affect the rheological properties of magnetic fluids. In addition, the study on the inner potential energy evolution of the magnetic fluid is also very important and attractive.

Molecular Dynamics (MD) is a form of computer simulation, which is used to model the configuration and property of a classical multi-body system based on Newton's laws of motion. It provides an effective way to determine mechanical behaviours of materials on the atomic scale. To our knowledge, the MD can be used to investigate microstructural evolution of magnetic fluids under a magnetic field [7–9]. However, the research on the relations between the mechanical

† Tel.: 86-551-3600419, fax: 86-551-3600419, e-Mail: gongxl@ustc.edu.cn

properties and microstructural evolution has not been performed. In this study, MD is introduced to investigate the structural and rheological characteristics of magnetic fluids, and the overall average stress formula [10] in an atomistic system is introduced to make mechanical analysis. Then the stress condition of magnetic fluids can be achieved based on the microstructures obtained by MD simulation.

This study aims to model and simulate the evolution process of three-dimensional microstructures in magnetic fluids under an external magnetic field when they are under shear or compression loadings. More importantly, the yield stresses and the evolution of potential energies under different conditions based on the microstructures are analyzed. The simulation results show that the yield stresses are enhanced with the magnetic field increasing or the increase of compressive strain, which is further verified by experimental studies. Moreover, the inner potential energy convert from dipole-dipole, particle-field magnetic energy and Van der Waals potential energy to repulsive potential energy with microstructural evolution under an external magnetic field was studied. The repulsive potential energy absorbs the work of external force making the compressive loading mostly. This research expands the cognition of magnetic fluids and is important for the magnetic fluid applications.

1. The simulation model and experimental.

1.1. The simulation model. The magnetic nanoparticles are taken as spherical particles, the diameters of which distribute from about 12 nm to 28 nm but with an average value of 20 nm, as Fig. 1*a* shows, dispersing in an incompressible Newtonian fluid medium of $\eta_s = 0.10\,\text{Pa·s}$ viscosity. The magnetic moments of the particles are determined by their volumes and the saturation magnetization of the materials making them immediately $m_i = M \cdot \pi d_i^3/6$ for particle i, where i is the mark number of a particle, d_i is the diameter of particle i, $M = 4.5 \times 10^5\,\text{A/m}$ is the saturation magnetization. The model system is a cubical box with edge length $L = 300\,\text{nm}$, containing about 5 vol. % of magnetic nanoparticles. In this study, as shows Fig. 1*b*, two simulations were carried out:

(A) One is concentrated on the study of the microstructure and rheological properties of magnetic fluids in a simple shear. The fluid is imposed by a simple shear flow with a shear rate $\dot{\gamma}$ along the x-direction, and the velocity increases linearly along the z-direction ($v = \dot{\gamma} z \cdot \hat{x}$).

(B) The other is to study magnetic fluid behaviours under a compression loading condition. The uniform compressive loading is along the z-direction. In both situations, an external magnetic field with a magnitude H is applied along the z-direction through the box. In order to simplify the simulations, the Stokes drag force is considered as the only hydrodynamic effect on the nanoparticles, while the gravity and buoyancy effects are neglected. The magnetic dipole interaction u_{ij}^{m}, the steric repulsive potential u_{ij}^{r} between the particles i and j and the particle-field interaction potential u_i^{h} are described as [1]:

$$u_{ij}^{\text{m}} = \frac{\mu_0 m_i m_j}{4\pi r_{ij}^3} \left[\mathbf{n}_i \cdot \mathbf{n}_j - 3\left(\mathbf{n}_i \cdot \mathbf{t}_{ij}\right)\left(\mathbf{n}_j \cdot \mathbf{t}_{ij}\right)\right], \tag{1}$$

$$u_{ij}^{\text{r}} = kT \frac{\pi\sigma d_{\text{a}}^2}{2} \left[2 - \frac{2r_{ij}}{\delta} \ln\left(\frac{d_{\text{a}} + 2\delta}{r_{ij}}\right) - \frac{r_{ij} - d_{\text{a}}}{\delta}\right], \tag{2}$$

$$u_i^{\text{h}} = -\mu_0 \mathbf{m}_i \cdot \mathbf{H}, \tag{3}$$

and the Van der Waals potential energy [11]:

$$u_{ij}^{\text{Van}} = -\frac{\text{A}}{6} \left[\frac{2}{L_{\text{r}}^2 + 4L_{\text{r}}} + \frac{2}{\left(L_{\text{r}} + 2\right)^2} + \ln\frac{L_{\text{r}}^2 + 4L_{\text{r}}}{\left(L_{\text{r}} + 2\right)^2}\right], \tag{4}$$

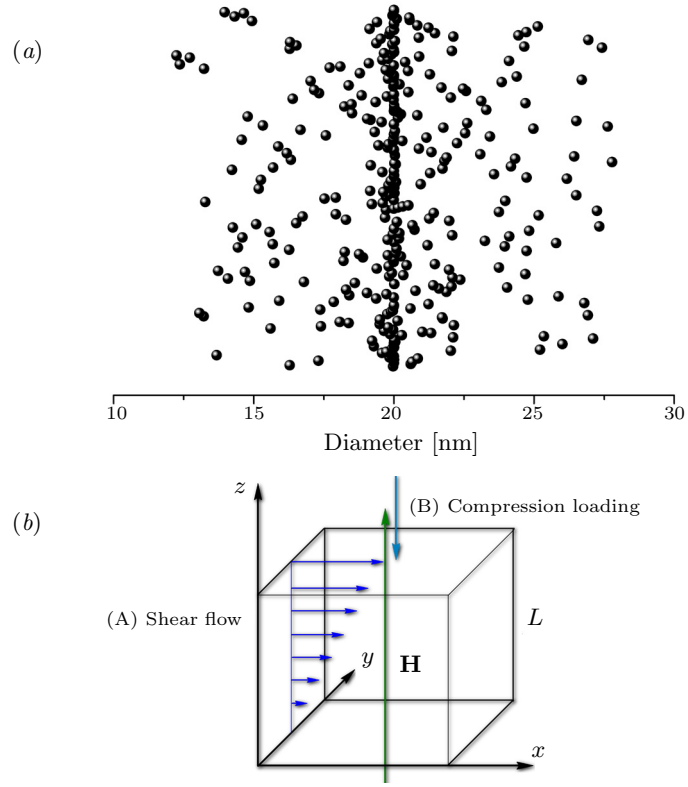

Fig. 1. (*a*) The sketch of the diameter distribution of particles. Each point sphere denotes a particle and the corresponding axis value refers to its diameter value. (*b*) Different loading modes are exerted on the considered box in the simulation.

with the vacuum permeability μ_0, the particle interdistance $\mathbf{r}_{ij} = \mathbf{r}_i - \mathbf{r}_j$, and $\mathbf{t}_{ij} = \mathbf{r}_{ij}/r_{ij}$, r_{ij} is the norm of vector $\mathbf{r}_{ij}$; $\mathbf{n}_i$ and $\mathbf{n}_j$ are the unit vectors denoting the direction of magnetic moments of particles i and j; $\sigma = 1.0 \times 10^{18}\,\mathrm{m}^{-2}$ is the surface concentration of absorbed molecules of the surfactant, and $\delta = 1.5 \times 10^{-9}\,\mathrm{m}$ is the thickness of the absorbed molecule $d_\mathrm{a} = (d_i + d_j)/2$, with d_i, d_j being the diameters of particle i and j, respectively; k is the Boltzmann constant, and $T = 298\,\mathrm{K}$ is the absolute temperature of the medium; A is the Hamaker constant, and $L_\mathrm{r} = 2(r_{ij} - d_\mathrm{a})/d_\mathrm{a}$. Furthermore, the magnetic dipole interaction force F_{ij}^m, the steric repulsive force F_{ij}^r, the particle-field force F_i^h and the Van der Walls interaction force F_{ij}^Van are obtained as

$$F_{ij}^\mathrm{m} = \frac{3\mu_0 m_i m_j}{4\pi r_{ij}^4}\Big[(\mathbf{n}_i \cdot \mathbf{n}_j)\,\mathbf{t}_{ij} - 5\,(\mathbf{n}_i \cdot \mathbf{t}_{ij})\,(\mathbf{n}_j \cdot \mathbf{t}_{ij})\,\mathbf{t}_{ij} + (\mathbf{n}_i \cdot \mathbf{t}_{ij})\,\mathbf{n}_i + (\mathbf{n}_i \cdot \mathbf{t}_{ij})\,\mathbf{n}_j\Big]\,, \tag{5}$$

$$F_{ij}^\mathrm{r} = kT\frac{\pi\sigma d_\mathrm{a}^2}{2\delta}\ln\left(\frac{d_\mathrm{a} + 2\delta}{r_{ij}}\right)\cdot t_{ij}\,, \tag{6}$$

$$F_i^\mathrm{h} = \mu_0\,(\mathbf{m}_i \cdot \nabla)\,\mathbf{H}\,, \tag{7}$$

$$F_{ij}^\mathrm{Van} = \frac{16\mathrm{A}}{(L_\mathrm{r} + 2)^3 \cdot (L_\mathrm{r}^2 + 4L_\mathrm{r})^2}\mathbf{t}_{ij}\,. \tag{8}$$

T_{ij}^{m} and T_i^{h} are the torques due to the dipole-dipole interaction and particle-field, respectively:

$$T_{ij}^{\mathrm{m}} = -\frac{\mu_0 m_i m_j}{4\pi r_{ij}^3}\left[\mathbf{n}_i \times \mathbf{n}_j - 3\left(\mathbf{n}_j \cdot \mathbf{t}_{ij}\right)\mathbf{n}_i \times \mathbf{t}_{ij}\right], \tag{9}$$

$$T_i^{\mathrm{h}} = \mu_0 \mathbf{m}_i \times \mathbf{H}. \tag{10}$$

Suppose that the nanoparticles initially randomly disperse in the box and their velocities are zero, then the translational and rotational motions are shown. For the particle i, the spatial position vector $\mathbf{r}_i(t)$ and the orientation vector of magnetic moment $\mathbf{n}_i(t)$ are described by the following equations [9]

$$\frac{\mathrm{d}\mathbf{r}_i}{\mathrm{d}t} = \frac{1}{\zeta_{\mathrm{t}}}\left[\sum_{j(j\neq i)}^{N}\left(F_{ij}^{\mathrm{m}} + F_{ij}^{\mathrm{r}} + F_{ij}^{\mathrm{Van}}\right) + F_i^{\mathrm{h}} + F_i^{\mathrm{b}}\right] + \dot{\gamma} z_i \hat{x}\,, \tag{11}$$

$$\frac{\mathrm{d}\mathbf{n}_i}{\mathrm{d}t} = \left[\frac{1}{\zeta_{\mathrm{r}}}\left(\sum_{j(j\neq i)}^{N} T_{ij}^{\mathrm{m}} + T_i^{\mathrm{h}} + T_i^{\mathrm{b}}\right) + \frac{\dot{\gamma}}{2}\hat{y}\right] \times \mathbf{n}_i\,, \tag{12}$$

with $\zeta_{\mathrm{t}} \equiv 3\pi d\eta_s$ being the translational drag force coefficient and $\zeta_{\mathrm{r}} \equiv \pi d^3\eta_s$ the rotational drag force coefficient, respectively; the stochastic or Brownian force F_i^{b} in equation (11) and the stochastic torque T_i^{b} in equation (12) obey the statistical thermal bath fluctuation rules [12]

$$\langle F_{i\phi}^{\mathrm{b}}(t)\rangle = 0\,, \quad \langle F_{i,\phi}^{\mathrm{b}}(t) F_{i,\chi}^{\mathrm{b}}(t')\rangle = 2kT\zeta_{\mathrm{t}} \cdot \delta_{ij}\delta_{\phi\chi}\delta(t'-t)\,, \tag{13}$$

$$\langle T_{i\phi}^{\mathrm{b}}(t)\rangle = 0\,, \quad \langle T_{i,\phi}^{\mathrm{b}}(t) T_{i,\chi}^{\mathrm{b}}(t')\rangle = 2kT\zeta_{\mathrm{r}} \cdot \delta_{ij}\delta_{\phi\chi}\delta(t'-t)\,. \tag{14}$$

Further, the overall average stress in the system, especially the shear stress $\bar{\sigma}_{xz}$ and the normal stress $\bar{\sigma}_{zz}$ along the magnetic field were calculated by [10]

$$\bar{\sigma}_{\alpha\beta} = \frac{1}{V}\sum_{k=1}^{n-1}\sum_{i\leq k}\sum_{j>k} F_{ij}\Delta r_k^z\,, \tag{15}$$

where F_{ij} is the interaction force between different layers; Δr_k^z is the interval of layers and n is the number of layers. The relative viscosity is obtained from the equation of

$$\eta_{\mathrm{eff}} = \frac{\bar{\sigma}_{xz}}{\dot{\gamma}}\,. \tag{16}$$

The above equations were numerically solved by the Euler method. The time step for the simulation was $\Delta t_0 = 2\times 10^{-7}$ s and the cutoff radius for the particle-particle interactions was taken as $r_{\mathrm{coff}} = 7d$. When calculating the shear stress in the system, we also took into account the effect of the Stokes drag force of the nanoparticles, which were suspended at the top of the fluid and attached to the moving plate due to the magnetic field force. Periodic boundary conditions were imposed in the x-and y-directions, and shear boundary conditions in the z-directions. The microstructure formation process and the corresponding average stress under different conditions were obtained by averaging the values of numerous calculations.

1.2. Experimental. In order to verify our simulation results in the shear condition, a magnetic fluid containing 5 vol. % magnetite nanoparticles was produced and its rheological property was measured, including the tests of the static yield stress and the shear stress when exposed to a steady shear flow. The experiment was conducted by an Anton Paar Physica MCR301 rheometer with a magnetorheological device, where the working condition was the same as that in MD simulation.

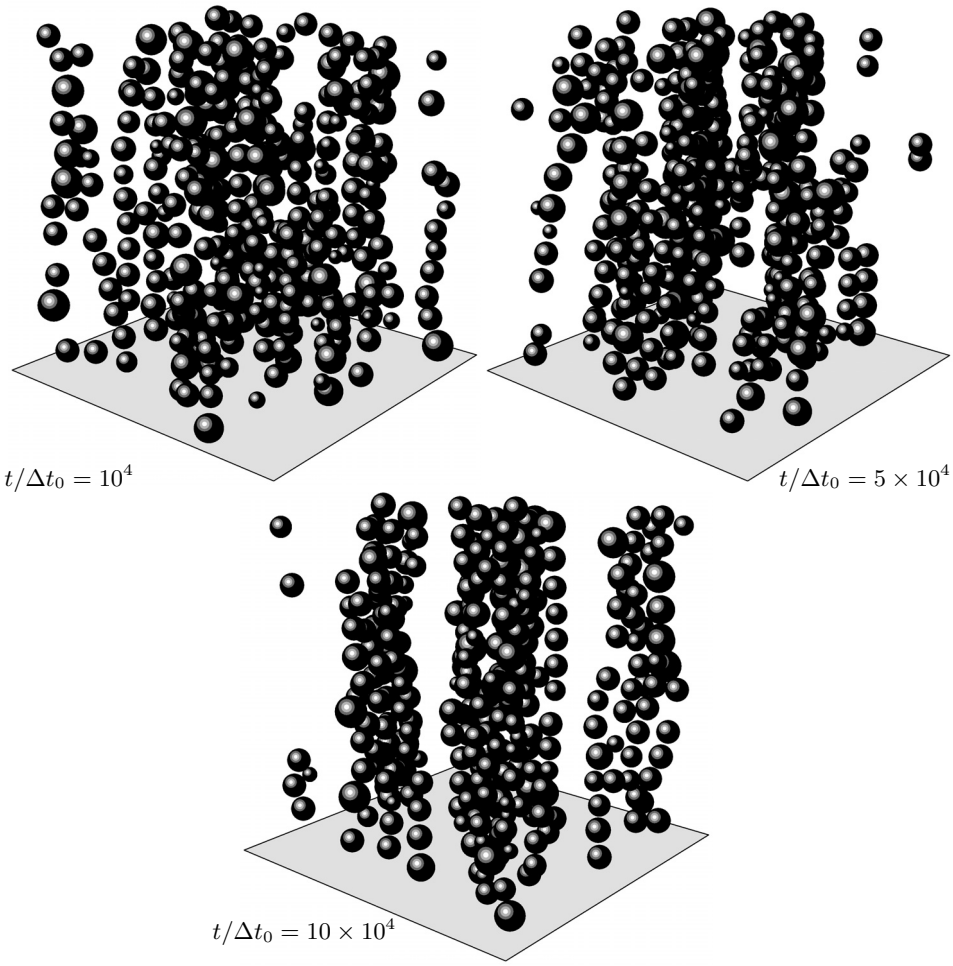

Fig. 2. Evolution of microstructures in magnetic fluids over time, while the magnetic field strength $H = 30\,\mathrm{kA/m}$ and shear rate $\dot{\gamma}$ is zero.

2. Results and discussions. The microstructures and stress state in the magnetic fluids without shears were discussed firstly. Fig. 2 shows the microstructure evolution over time when the shear rate is zero. It is obvious that the magnetic dipole nanoparticles would aggregate into chain-like structures and then merge into column-like structures with time under an externally applied magnetic field. This result has proven that the magnetic fluids are thermodynamically and hydrodynamically instable; also, the interaction force between different chains is much weaker than that in the same chain. Fig. 3 shows the evolution of potential energy densities over time. It can be seen that the magnetic field energy u^{h}, magnetic dipole energy u^{m} and the Van der Waals potential energy u^{Van} decrease at first and then keep stable with time, while u^{h} goes down especially drastically. At the same time, the repulsive potential energy u^{r} increases suddenly and becomes a constant. It is deduced that the decreasing potential energies u^{m}, u^{h} and u^{Van} convert to u^{r} and inner friction consumption. The time for the overall energy stabilization is about 1.5 ms. In order to ensure the microstructures and their rheological properties in a relatively stable situation, all the integral time of the following simulation is $t = 10^5 \Delta t_0 \approx 20\,\mathrm{ms}$.

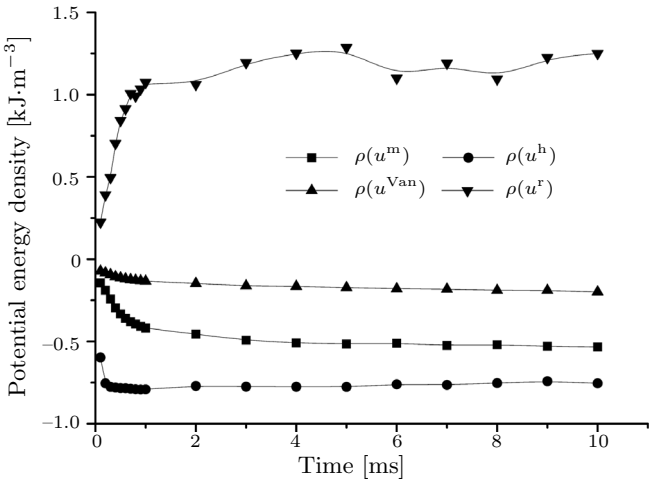

Fig. 3. Variation of potential energy density in the system over time, with $\rho(u^{\mathrm{m}})$, $\rho(u^{\mathrm{h}})$, $\rho(u^{\mathrm{Van}})$ and $\rho(u^{\mathrm{r}})$ being the densities of magnetic dipole energy, magnetic field energy of particles, Van der Waals potential energy and the repulsive potential energy of interacting particles, respectively.

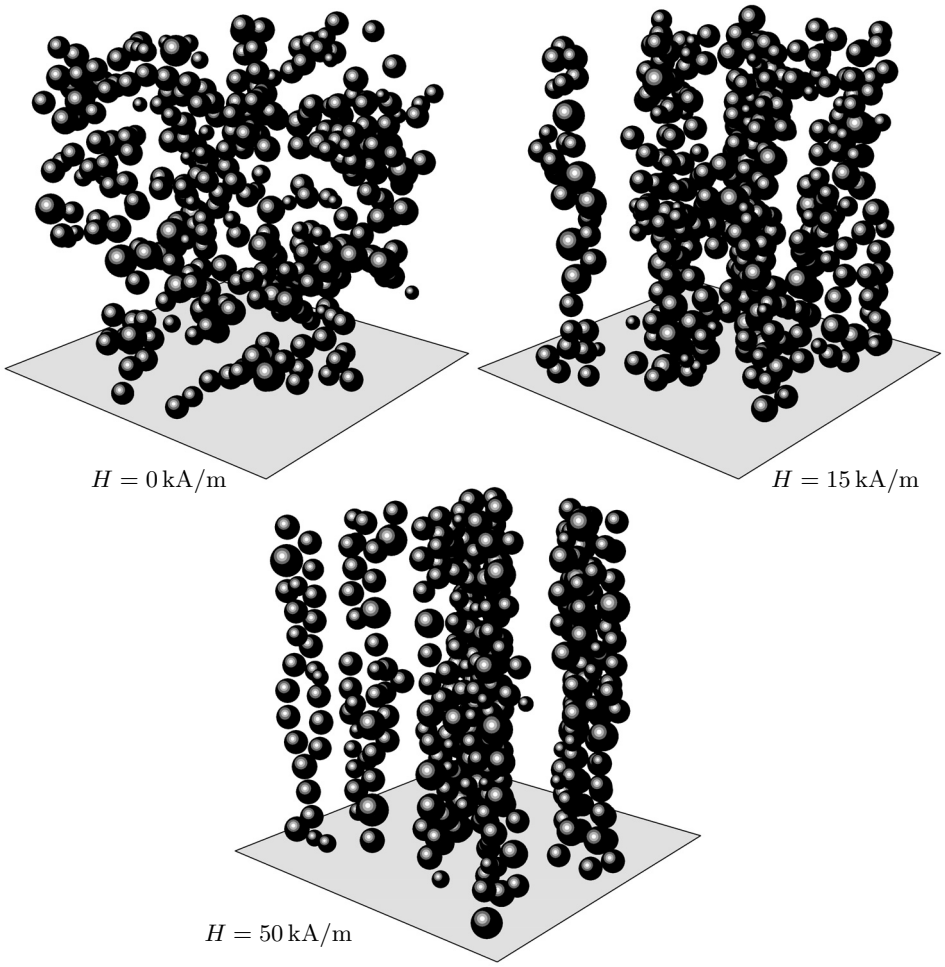

Fig. 4. The microstructure of magnetic fluids goes along with the increase of magnetic field.

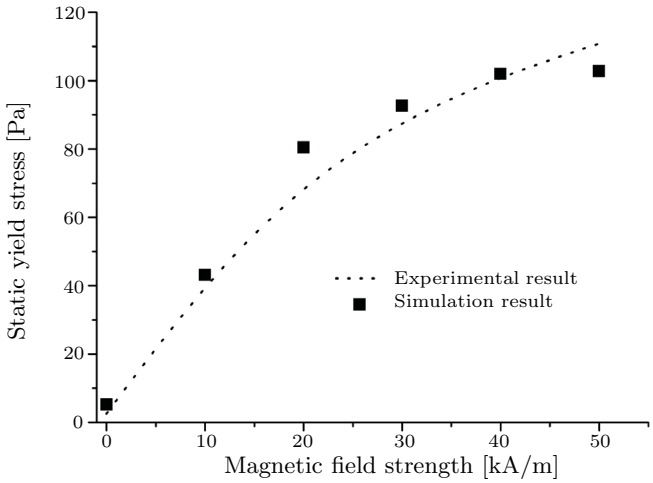

Fig. 5. The static yield stress as a function of the magnetic field strength in magnetic fluids.

Fig. 4 illustrates the microstructures of magnetic fluids under different magnetic fields in the static state. Without the external magnetic field, the nanoparticles with random magnetic moments would form a flocculent-like aggregation due to their dipole-dipole interactions; when the magnetic field is turned on, the particles form chain-like aggregates and these structures are strengthened by the increasing magnetic field strength. The average force f_{p} parallel to the z-direction per unit horizontal area in the suspension was obtained from the average stress formula, and the static yield stress τ_y was obtained from the relationship $\tau_y = f_p{\cdot}\sin\theta$, where θ is the inclination angle when the structure is affected by a shear. Thus, the relationship between the static yield stress and the magnetic field strength has been obtained. Fig. 5 shows the simulation results (when $\theta \approx 16.5^\circ$ and their comparison with experimental results. The simulation results generally agree with the experimental ones – the static yield stress increases with the enhancement of the magnetic field strength. The results of Figs. 4 and 5 demonstrate that the more compact the chain-like structures, the greater the static yield stress.

The following simulations are for the microstructural and rheological properties of the magnetic fluids imposed by a simple steady shear flow. Fig. 6 illustrates the variation of microstructures with different shear rates under a magnetic field. By comparing the three sets of images, it is clear that the chain-like and column-like aggregates disperse randomly when $\dot{\gamma}$ is very small, while they gradually incline towards the x-direction with the increase of $\dot{\gamma}$, for the velocity field linearly increases along the z-direction. When $\dot{\gamma}$ is large enough, the magnetic aggregates evolve into lamellar patterns, which are parallel to the x-direction, and these changes are attributed to the effects of the Stokes drag force driven by the shear flow. Fig. 7 shows that the inner potential energies evolve with the shear rate sweep. With the shear rate increase, u^{m}, u^{Van} originally decrease and then keep stable; u^{h} increases slowly, but u^{r} increases rapidly when the shear rate is lower than $1.5\,\mathrm{s}^{-1}$ and then shows period changing with a small amplitude. The increasing energy of u^{r} absorbed the work of external force making the shear flow and then was consumed to drive the motion of particles to aggregate new structures.

Fig. 8 shows the flow curve of the magnetic fluids at the constant magnetic field strength $H = 30\,\mathrm{kA/m}$. The shear stress increases linearly with the increasing shear rates, which could be described by the 'Bingham model'; the relative viscosity

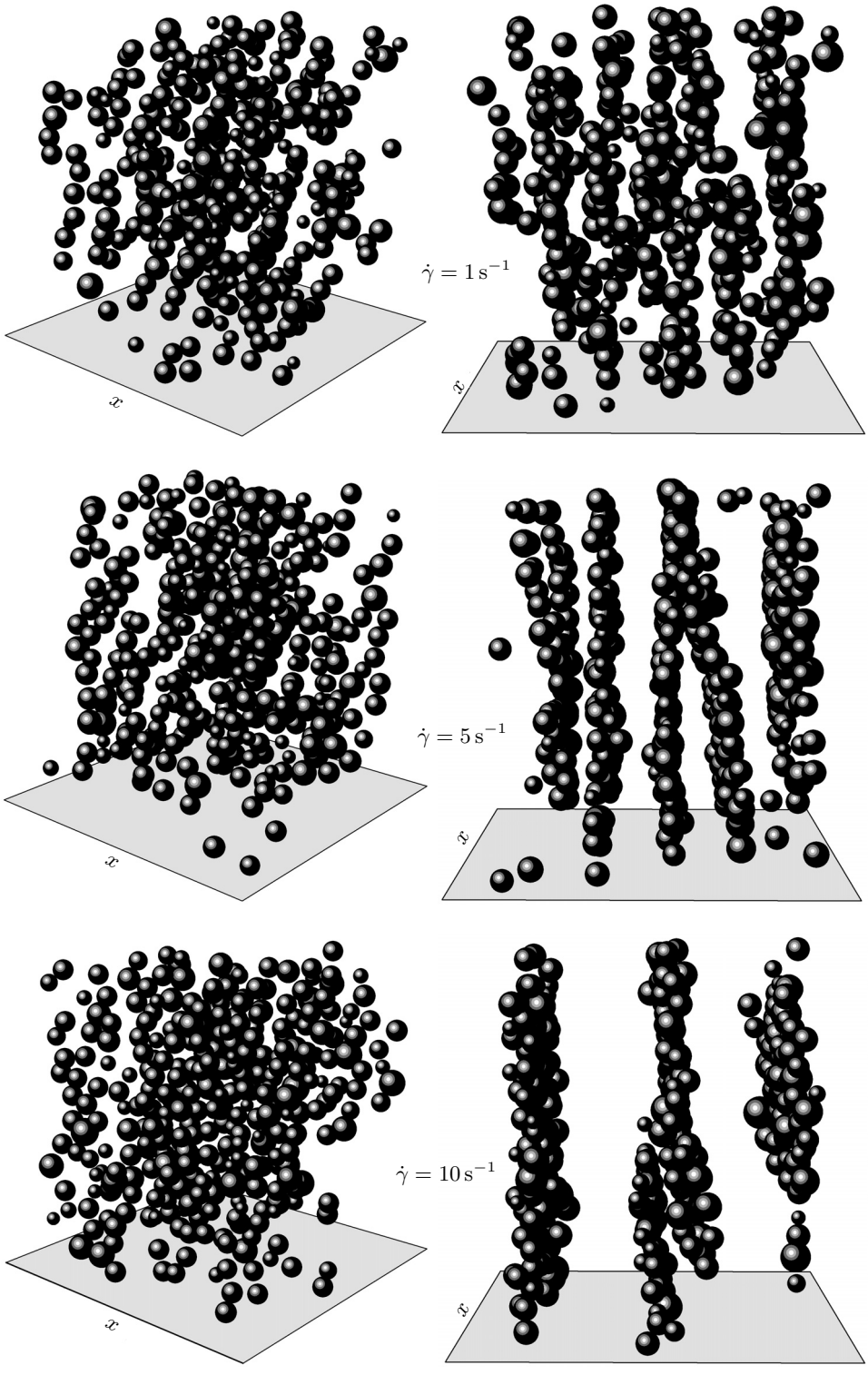

Fig. 6. Microstructures in magnetic fluids for different shear rates when $H = 30\,\mathrm{kA/m}$; the left and right figures in each set are the images observed three-dimensional and perpendicular to the shear flow, respectively.

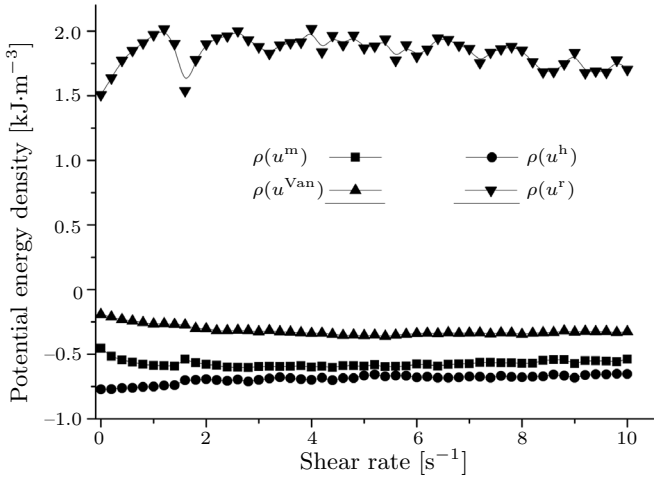

Fig. 7. Variation of the potential energy density over the shear rate.

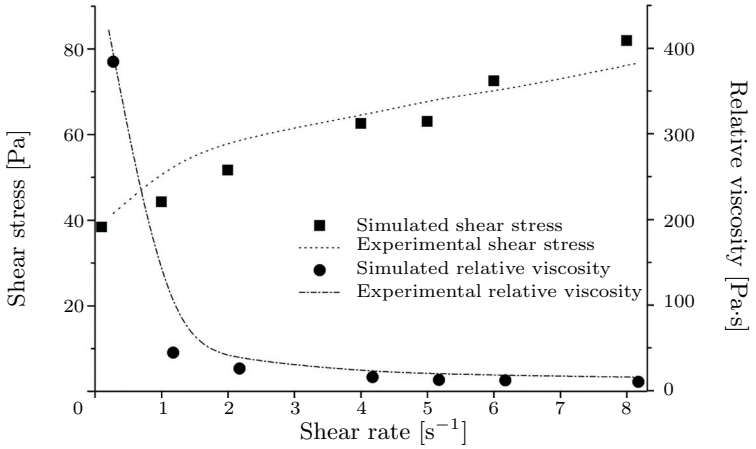

Fig. 8. The shear stress and relative viscosity as a function of shear rates in magnetic fluids when $H = 30\,\mathrm{kA/m}$.

steeply declines when $\dot{\gamma}$ is small ($\dot{\gamma} < 2\,\mathrm{s}^{-1}$) and then comes to a relatively small constant (approximately $\epsilon_\infty = 9.5\,\mathrm{Pa{\cdot}s}$) when $\dot{\gamma}$ becomes more than $5\,\mathrm{s}^{-1}$. The simulation values basically coincide with the experimental results as shown in Fig. 8. By comparing the results of Figs. 6 and 8, it could be deduced that when the nanoparticles aggregate into lamellar structures in such a large shear, the viscosity resistances, to which the structures are subjected, would reduce and the relative viscosity of the suspension would decrease, accordingly.

From the above results, we can conclude that the thick and compact column-like aggregates along the magnetic field may give rise to a strong yield stress in magnetic fluids. Similar conclusions in the MR fluid experimental research have been drawn. The MR fluids under compression exhibit a strongly enhanced MR effect, where the yield stress is more than 10 times higher if compared to conventional MR fluids [13–14]. We would like to extend this approach to magnetic fluids. It is expected that the compression of magnetic fluids would result in much stronger microstructures in them.

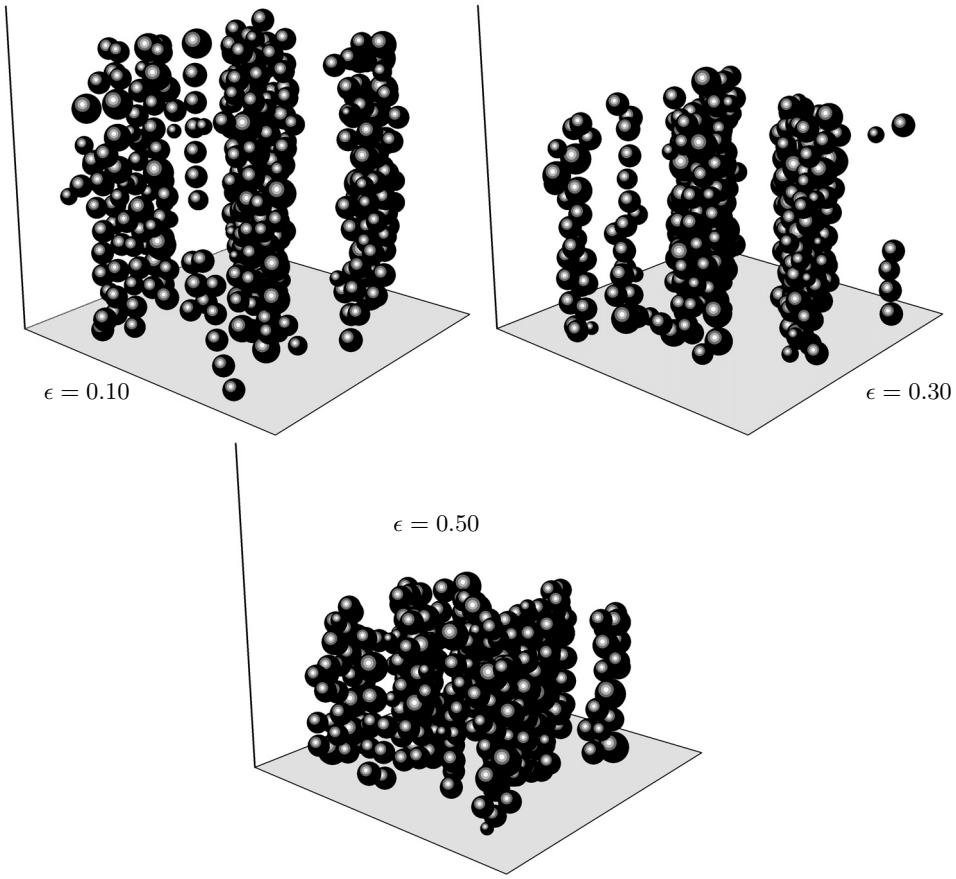

Fig. 9. Microstructures in magnetic fluids under compression loading when $H = 30\,\mathrm{kA/m}$ and $\dot{\epsilon} = 3.1\,\mathrm{s}^{-1}$.

Fig. 9 show the microstructures of magnetic fluids under three typical compression strains of 0.10, 0.30 and 0.50, respectively. Obviously, the chain-like aggregates become much thicker and more compact columns with the increase of the compressive strain along the field direction. Since the yield stress is proportional to the average normal stress along the magnetic field direction, the relationship between yield stress and compressive strain under a uniform compression loading was obtained. Fig. 10 shows the relations between the relative yield stress and the compressive strain at different compressive rates, where the relative yield stress is the ratio of static yield stress under compression to that without compression. It can be seen from Fig. 10 that the relative yield stress grows significantly with the increase of compressive strain when the compressive rate $\dot{\epsilon}$ is a constant. This result indicates that magnetic fluids under compression loadings would lead to a stronger yield strength. Moreover, values of the relative yield stress also increase with the compressive rate, which demonstrate that the chain-like structures under quick compression in the magnetic fluid would tend to form more rigid column-like structures. Fig. 11 shows that u^{r} increases quickly with the enhancement of strain, while the values of u^{h}, u^{m}, u^{Van} keep constant. Hence, u^{r} absorbs the work of compression loading mostly, then forces the aggregation structures to change into thicker columns so enhancing the yield stress of magnetic fluids.

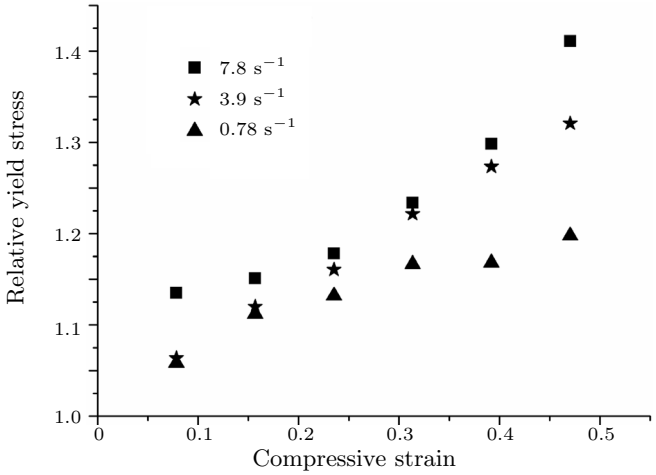

Fig. 10. The relative yield stress in magnetic fluids as a function of compressive strain.

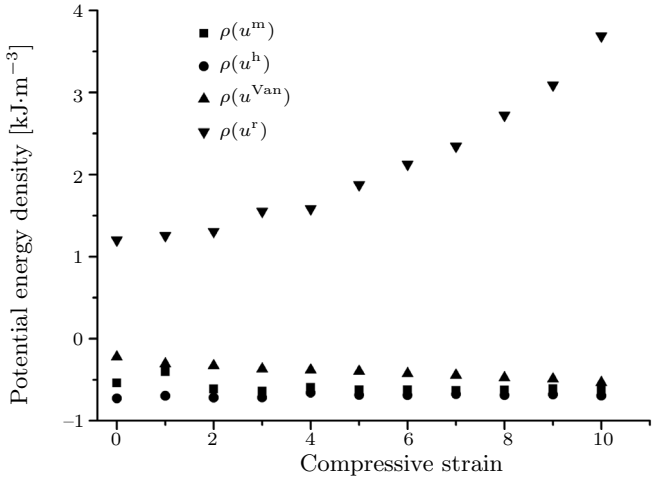

Fig. 11. Variation of potential energy densities in the system over compressive strain when $H = 30\,\mathrm{kA/m}$ and $\dot{\epsilon} = 3.1\,\mathrm{s}^{-1}$.

3. Conclusion. In this work, the microstructures and the rheological properties of magnetic fluids exposed to an external magnetic field under shear and compression loading are studied by molecular dynamics simulation. The inner potential energies are investigated for their microstructure evolutions. The simulation stress in the shear condition coincides fairly with the experimental ones, which proves that MD is an effective method to investigate the rheological properties of magnetic fluids. The simulation results indicate that the magnetic nanoparticles would aggregate into chain-like microstructures under a magnetic field; these structures might be strengthened with the enhancement of field density, so that the static yield stress increases at the same time. The potential energy decrease of particle-particle, particle-field and Van der Waals interactions contributes to the increase of repulsive potential energy and the inner friction consumption. Steady shear motion may rearrange the one-dimensional structures into lamellar patterns along the shear, which could bear small viscosity friction in a large shear, therefore, the relative viscosity of magnetic fluids decreases. On the other hand, magnetic

fluids under compression loadings would result in more compact microstructures and consequently lead to enhanced yield stresses. This research is important to expand the cognition and for the application of magnetic fluids.

Acknowledgements. Financial support from the National Basic Research Program of China (973 Program, Grant No. 2007CB936800) is gratefully acknowledged.

REFERENCES

[1] R.E. Rosensweig. *Ferrohydrodynamics* (Cambridge University Press, New York, 1985).

[2] S. Sun, C.B. Murray, D. Weller, L. Folks, A. Moser. Monodisperse FePt nanoparticles and ferromagnetic FePt nanocrystal superlattices. *Science*, vol. 287 (2000), no. 5460, pp. 1989–1992.

[3] K.E. Scarberry, E.B. Dickerson, J.F. McDonald, Z.J. Zhang. Magnetic nanoparticle-peptide conjugates for in vitro and in vivo targeting and extraction of cancer cells. *J. Amer. Chem. Soc.*, vol. 130 (2008), no. 31, pp. 10258–10262.

[4] C.Y. Chen, W.K. Tsai, J.A. Miranda. Experience study of a hybrid ferrohydrodynamic instability in miscible ferrofluids: droplet size effects. *Magnetohydrodynamics*, vol. 45 (2009), no. 1, pp. 3–14.

[5] A.Yu. Zubarev, L.Yu. Iskakova. Yield stress in ferrofluids. *Magnetohydrodynamics*, vol. 43 (2007), no. 1, pp. 3–15.

[6] L.M. Pop, S. Odenbach, A. Wiedenmann. Microstructure and rheology of ferrofluids. *J. Magn. Magn. Mater.*, vol. 289 (2005), pp. 303–306.

[7] G.N. Coverdale, R.W. Chantrell, A. Satoh, R. Vietch. Molecular dynamic model of the magnetic properties and microstructure of advanced metal particle dispersions. *J. Appl. Phys.*, vol. 81 (1997), no. 8, pp. 3818–3820.

[8] V.V. Murashov, G.N. Patey. Structure formation in dipolar fluids driven by rotating fields. *J. Chem. Phys.*, vol. 112 (2002), no. 22, pp. 9828–9833.

[9] Y. Enomoto, K. Oba, M. Okada. Simulation study on microstructure formations in magnetic fluids. *Physica A.*, vol. 330 (2003), no. 3, pp. 496–506.

[10] Z.H. Sun, X.X. Wang, A.K. Song, H.A. Wu. On stress calculations in atomistic simulations. *Modell. Simul. Mater. Sci. Eng.*, vol. 14 (2006), no. 3, pp. 423–431.

[11] W.B. Russel, D.A. Saville, W.R. Schowalter. *Colloidal Dispersion* (Cambridge University Press, 1989).

[12] D.V. Berkov, N.L. Gorn, R. Schmitz, D. Stock. Langevin dynamic simulations of fast remagnetization processes in ferrofluids with internal magnetic degrees of freedom. *J. Phys.: Condens. Matter.*, vol. 18 (2006), no. 38, pp. 2595–2621.

[13] X. Tang, X. Zhang, R. Tao, Y.M. Rong. Structure-enhanced yield stress of magnetorheological fluids. *J. Appl. Phys.*, vol. 87 (2000), no. 5, pp. 2634–2638.

[14] X.Z. Zhang, X.L. Gong, P.Q. Zhang. Study on the mechanism of the squeeze-strengthen effect in magnetorheological fluids. *J. Appl. Phys.*, vol. 96 (2004), no. 4, pp. 2359–2364.

Received 13.09.2010